Simulating Climate Change and Socio-economic Change Impacts on Flows and Water Quality in the Mahanadi River System, India

Li Jin[1*], Paul G. Whitehead[2], Harvey Rodda[3], Ian Macadam[4], Sananda Sarkar[5]

[1] Geology Department, State University of New York College at Cortland, Cortland, NY 13045, USA

[2] School of Geography and the Environment, University of Oxford, Oxford, UK

[3] Hydro-GIS Ltd, 10 Coles Lane, Chalgrove, Oxfordshire OX44 7SY, UK

[4] Met Office, FitzRoy Road, Exeter, EX1 3PB, United Kingdom

[5] School of Civil Engineering, Kalinga Institute of Industrial Technology, Bhubaneswar, Odisha 752024, India

* Li Jin li.jin@cortland.edu

Abstract

Delta systems formed by the deposition of sediments at the mouths of large catchments are vulnerable to sea level rise and other climate change impacts. Deltas often have some of the highest population densities in the world and the Mahanadi Delta in India is one of these, with a population of 39 million. The Mahanadi River is a major river in East Central India and flows through Chattisgarh and Orissa states before discharging into the Bay of Bengal. This study uses an Integrated Catchment Model (INCA) to simulate flow dynamics and water quality (nitrogen and phosphorus) and to analyze the impacts of climate change and socio-economic drivers in the Mahanadi River system. Future flows affected by large population growth, effluent discharge increases and changes in irrigation water demand from changing land uses are assessed under shared socio-economic pathways (SSPs). Model results indicate a significant increase in monsoon flows under the future climates at 2050s (2041-2060) and 2090s (2079-2098) which greatly enhances flood potential. The water availability under low flow conditions will be worsened because of increased water demand from population growth and increased irrigation in the future. Decreased concentrations of nitrogen and phosphorus are expected due to increased flow hence dilution. Socio-economic scenarios have a significant impact on water quality but less impact on the river flow. For example, higher population growth, increased sewage treatment discharges, land use change and enhanced atmospheric deposition would result in the deterioration of water quality, while the upgrade of the sewage treatment works lead to improved water quality. In summary, socio-economic scenarios would change future

water quality of the Mahanadi River and alter nutrient fluxes transported into the delta region. This study has serious implications for people's livelihoods in the deltaic area and could impact coastal and Bay of Bengal water ecology.

Key Words: flow, nitrogen, phosphors, climate change, socio-economic changes, modeling

Introduction

River discharge, nutrient load and sediment load of most of the world's largest rivers have experienced great changes in recent decades and are vulnerable to future changes due to the variations of climate and anthropogenic impacts around the globe (Bastia and Equeenuddin, 2016; Hoang et al., 2016; Jin et al., 2015; Walling, 1997; Walling and Fang, 2003; Whitehead et al., 2015a; Whitehead et al., 2015b). The delta systems forming from deposition of sediments at the mouths of these large river catchments are therefore unavoidably affected by these changes (Eldeberky and Hunicke, 2015; Immerzeel, 2008; Kay et al., 2015; Lazar et al., 2015; Nicholls et al., 2016; Smajgl et al., 2015; Susnik et al., 2015; Whitehead et al., 2015a). Deltas have some of the highest population densities and often poor residents in the world. These low-elevation coastal areas are experiencing loss of livelihood from climate change induced risks of flooding, storm surges and sea-water intrusion (Hoang et al., 2016; Sherif and Singh, 1999; Van et al., 2012; Vastila et al., 2010; Whitehead et al., 2015a). Therefore, it is crucial to analyze the impacts of climate change and other environmental drivers in these large rivers and deltas and to develop strategies and policies that are adaptive to deltas residents.

Climate can significantly affect the hydrological conditions and water resources arising from change in precipitation intensity and frequency, which have resulted in extensive flooding and extended drought (IPCC, 2007, 2013). Additionally, socio-economic change such as urbanization and population increase have put additional stress on water resources which can worsen the issues of water scarcity and food production (IPCC, 2014). Although climate change is occurring globally, impact is likely to be severe in countries like India due to their agricultural-based rural economy. In India, over two-thirds of the population directly depends on agriculture which is largely controlled by rainfall due to south-west summer monsoon for the period of June to October. Any change in climate such as variability in the monsoon would significantly affect the agriculture and food security. In addition, India has experienced a significant increase in water demand over the years because of increasing population. According to the United Nations Environment Programme (UNEP) (Global Environment Outlook, 2000), if the consumption patterns continue, by the year 2025, India may be under high water stress (more than 40% of total available utilized). Given the circumstances, the country is presently facing water stress which is likely to worsen under climate and socio-economic changes.

This study, as part of DECCMA (DEltas, vulnerability and Climate Change: Migration and Adaptation) project (Hill et al., 2018), will focus on the Mahanadi River, one of the largest peninsular rivers in India. There have been a number of studies in the past which evaluated streamflow (including floods) change under changing climate in the Mahanadi River. For example, a study by P.G. Rao (1995) showed climate warming occurred in the Mahanadi River basin and a steady decrease in the river flows during the 55-year period of the study (1926-1980) (Rao, 1995). Later, General Circulation Models (GCMs) output with 150km resolution were used and downscaled by a statistical method to assess the flow changes in the Mahanadi river basin (Ghosh et al., 2010). In this study, we have downscaled three GCMs from the most recent (CMIP5) generation of GCMs. These GCMs have been carefully selected by Janes et al. (2018) to sample a broad range of plausible future climate change scenarios for northern India. In addition to using more up to date GCMs than Ghosh et al. (2010), we use data dynamically downscaled to a resolution of 25km from the GCMs. The dynamical downscaling was done using a Regional Climate Model (RCM), which better represents fine scale processes that are important for determining regional climate conditions than a GCM.

We seek to address flow and water quality issues related to nitrogen (N) and phosphorus (P) in the Mahanadi River and nutrient transport along the river and discharge into the delta system. We evaluate the impact on flow and water quality from climate and socio-economic change utilizing a modelling approach as a means of assessment in this complex river system. The INCA-N and INCA-P models have been applied to the Mahanadi River system to simulate flow and water quality along the rivers under a range of future conditions. This is the first study which uses applications of the INCA models in the Mahanadi River basin to assess both climate change and socio-economic change on water resource systems. Considering both flow and water quality can assist catchment management in a more holistic way. This study emphasizes the need for groundbreaking water management policies to mitigate flooding and drought conditions and impacts on the deltaic environment.

Study Area

The Mahanadi is a major east-flowing peninsular river in east-central India (Figure 1a). Extending between the longitudes of 80°28'E to 86°43'E and latitudes of 19°8'N to 23°32'N, the Mahanadi River system has a coverage area of 141,589 km^2. It is approximately 4.3% of the total geographical area of India, with the major part of the basin covering the state of Orissa and Chhattisgarh and the rest in the states of Jharkhand, Maharashtra and Madhya Pradesh. The basin is bounded by the Central India Hills on the north, the Eastern Ghats on the south and east and the Maikala range on the west. Geologically the basin comprises of pre-Cambrian hard rock in the upstream reaches and alluvium formation of recent origin in the downstream reaches.

The Mahanadi River is 851 km in length and originates in Pharsiya village in the Dhamtari district of Chhattisgarh. The river drains into the Mahanadi Delta on the east coast of the Bay of Bengal (Figure 1b). The left bank tributaries of the Mahanadi River are the Seonath, the Mand, the Ib and the Hasdeo, whereas the right bank tributaries include the Rivers Ong, the Jonk and the Tel.

The river course is considered to be divided into 3 sections. Upper Mahanadi originates from a combination of many mountain streams and then flows towards north as a small stream in the plain of Chhattisgarh until it is joined by the River Seonath near Seorinarayan. From its confluence with the Seonath, the river takes an easterly course to enter into the state of Odisha forming Middle Mahanadi. Near the city of Sambalpur, the river flows into a large artificial Hirakud reservoir of capacity 743 km^2 under full conditions created by a 25.8 km long earthen dam (including dykes) of the same name. Below the dam the Mahanadi follows a meandering course through deep, forested ridges and forces its way through the Eastern Ghats via the 64 km long Satkosia Gorge. The Lower Mahanadi enters the Orissa plains leaving the hilly region at Naraj. A barrage has been constructed here to control flooding in the lower sections. At Cuttack, the Mahanadi splits into several branches (or distributaries) that finally discharges into the Bay of Bengal. The delta formed at the mouth of the river is a very fertile agricultural plain and densely populated.

The climate of the basin is sub-tropical in nature with maximum temperatures ranging from 39 °C to 45 °C occurring in the month of May and minimum temperature varying from 4 °C to 12 °C during the winter month of December to January. The mean annual rainfall is about 1200 mm with 90% of the rainfall falling in the monsoon months of June to October. The distribution of rainfall is uneven over the Mahanadi basin. Drought is prevalent in some districts, while severe flooding due to the heavy precipitation during the monsoon often disrupts life in the delta area.

Agriculture and forest are two main land uses in the basin (Figure 1c). The principal soil types in the basin are red and yellow soils, mixed red and black soils, laterite soils and deltaic soils. The important urban centers located along the course of the rivers are Raipur, Sambalpur, Sonepur, Boudh, Cuttack, Paradip and etc (Figure 1b). As per the 2011 census, the approximate population in the basin is 38.6 million, an increase by 1.9% from 2001 (Forum for Policy Dialogue on Water Conflicts in India (2017).

The Mahanadi is a great source of water for irrigation, industry, domestic utilities and for producing hydroelectricity. The average water resource potential of Mahanadi is 66.9 km^3 out of which 50 km^3 is of usable surface water potential (Central Water Commission, 2014). In the Mahanadi basin, around 253 dams and 27 barrages/weirs have been constructed to support 63 irrigation projects and 5 hydroelectric projects (Mahanadi Basin Report, WRIS, 2014).

In addition, 11 new irrigation projects are ongoing in response to the rapidly growing water demand due to urbanization and industrialization. As a result, the river is under the serious threat of reduced flows during the dry period.

The two main sources of pollution in the Mahanadi River are identified as (i) households and municipal untreated sewage disposal sites and (ii) effluents from commercial activity or industrial sites. The Orissa Pollution Control Board (OSPCB) estimates the cities in the Mahanadi basin generate about 345,000 m^3 of raw domestic sewage every day. Effluents from the Phosphatic Fertilizer Industry at Paradeep contains toxic chemicals like nitric, sulfuric, phosphatic acids and ammonia. They are polluting the delta reaches of the Mahanadi before flowing into the Bay of Bengal. In the Mahanadi basin, several medium and small scale industries produce about 100,000 m^3 of waste water/day on average. However, the entire amount is not released into the river as major part of them is diverted to marshland. The mining activities in the coal mines located in Ib valley generate about 14,000 m^3/day of waste water. Besides, the chemical wash-off from fertilizers and pesticides used in agricultural fields, human activities like immersion of idols during religious festivals and open defecation pose grave threat to the very existence of the Mahanadi River.

INCA Models and PERSiST

The Integrated Catchment Model (INCA) was first created by Whitehead et al., 1998 and then has been widely applied to many different river systems around the world (Barlund et al., 2009; Flynn et al., 2002; Futter et al., 2007; Hadjikakou et al., 2011; Jin et al., 2016; Jin et al., 2015; Lazar et al., 2010; Ranzini et al., 2007; Wade et al., 2002; Whitehead et al., 2011; Wilby et al., 2006). INCA model is process-based and simulates flow and water quality (e.g. Nitrogen, Phosphorus, Chloride, Carbon, Metals, Sediment and Organic Contaminants) in soil, groundwater and streams (Futter et al., 2007; Jackson-Blake et al., 2016; Jin et al., 2011; Lazar et al., 2010; Lu et al., 2017; Wade et al., 2002; Whitehead et al., 2009; Whitehead et al., 2011). Among INCA family models, INCA-Nitrogen(INCA-N) and INCA-Phosphorus (INCA-P) are especially used extensively (Crossman et al., 2013; Futter et al., 2009; Hadjikakou et al., 2011; Jarvie et al., 2002; Jin and Whitehead, 2010; Jin et al., 2016; Jin et al., 2015; Lazar et al., 2010; Wade et al., 2002; Whitehead et al., 2011). INCA is semi-distributed and takes account of spatial variations in land use, vegetation and hydrology by dividing the catchment into subcatchments (Wade et al., 2002; Whitehead et al., 1998). One of the essential updates to the N and P models is the multi-branch structure in which distributed river networks can be simulated (Whitehead et al., 2011). It greatly improved the simulation for large and complex river systems (Jin et al., 2015; Whitehead et al., 2015a). A detailed generic INCA model structure description can be found in Whitehead et al. (2011).

All versions of the INCA models operate on a daily time step and are based on a series of interconnected differential equations that are solved using numerical integration method with the fourth-order Runge-Kutta technique (Jackson-Blake et al., 2016; Lazar et al., 2010; Wade et al., 2002; Whitehead et al., 1998).

In order to run an INCA model, input data are required including river network topology, reach characteristics, sub-catchment areas, land use, hydrological parameters including rainfall, temperature, hydrologically effective rainfall (HER) and soil moisture deficits (SMD). HER and SMD were generated by the PERSiST model (Futter et al., 2014; Futter et al., 2015). PERSiST is a watershed-scale hydrological model and it is a conceptual, daily time-step, semi-distributed model designed primarily for use with the INCA models. INCA model calibration is generally undertaken using a combination of field observation and measurements, literature values, professional judgment and statistical analysis.

INCA-N is a process-based model which simulates flow and nitrate (NO_3-N) and ammonium (NH_4-N) concentrations in soil, streams and groundwater (Wade et al., 2002; Whitehead et al., 1998). The model divides the water course into multiple reaches with associated subcatchments, which are further grouped into different land uses. The model tracks N inputs which flow into the river from throughout the catchment by accounting for diffuse source input (e.g. fertilization application and atmospheric deposition) and point effluent input (e.g. sewage discharge). The model includes all key biochemical processes. Fluxes and concentrations of N are simulated by solving mass balance equations for terrestrial processes whilst simultaneously solving flow equations which determine the runoff and the infiltration into the ground and river channels as well as the dilution potential of the river (Wade et al., 2002).

INCA-P uses the same model structure as INCA-N by simulating flow from HER through the soil from different land use types to deliver P to the river system, which is then moved downstream after accounting for point sources (e.g., effluent discharges) and in-stream processes. It tracks stores and fluxes of water and P in both the land and in-stream phases of a river catchment from a hydrological module, a sediment module, a land phase P module and an in-stream P module (Jackson-Blake et al., 2016). Typical P inputs to the model consist of atmospheric depositions, fertilizer applications and sewage treatment effluents.

Applications of INCA models to Mahanadi River

The INCA-N (version 1.0.16) and the INCA-P (version 1.4.11) models have been applied to the entire Mahanadi River system. The river has been divided into 10 reaches (Figure 1b and 1c). The reach boundaries were selected based on the locations of the tributary confluences, the key flow and water quality monitoring stations, major cities, and the waste water treatment effluent inputs or abstraction points. Then associated subcatchments for each reach were delineated using the Digital Terrain Map (DEM) in ArcGIS. Subcatchment characteristics were obtained from the DEM and land cover maps including subcatchment area and percentage land use (Table 1). The six land uses considered are water, forest, grassland, wetland, cropland and urban (Table 1 and Figure 1c).

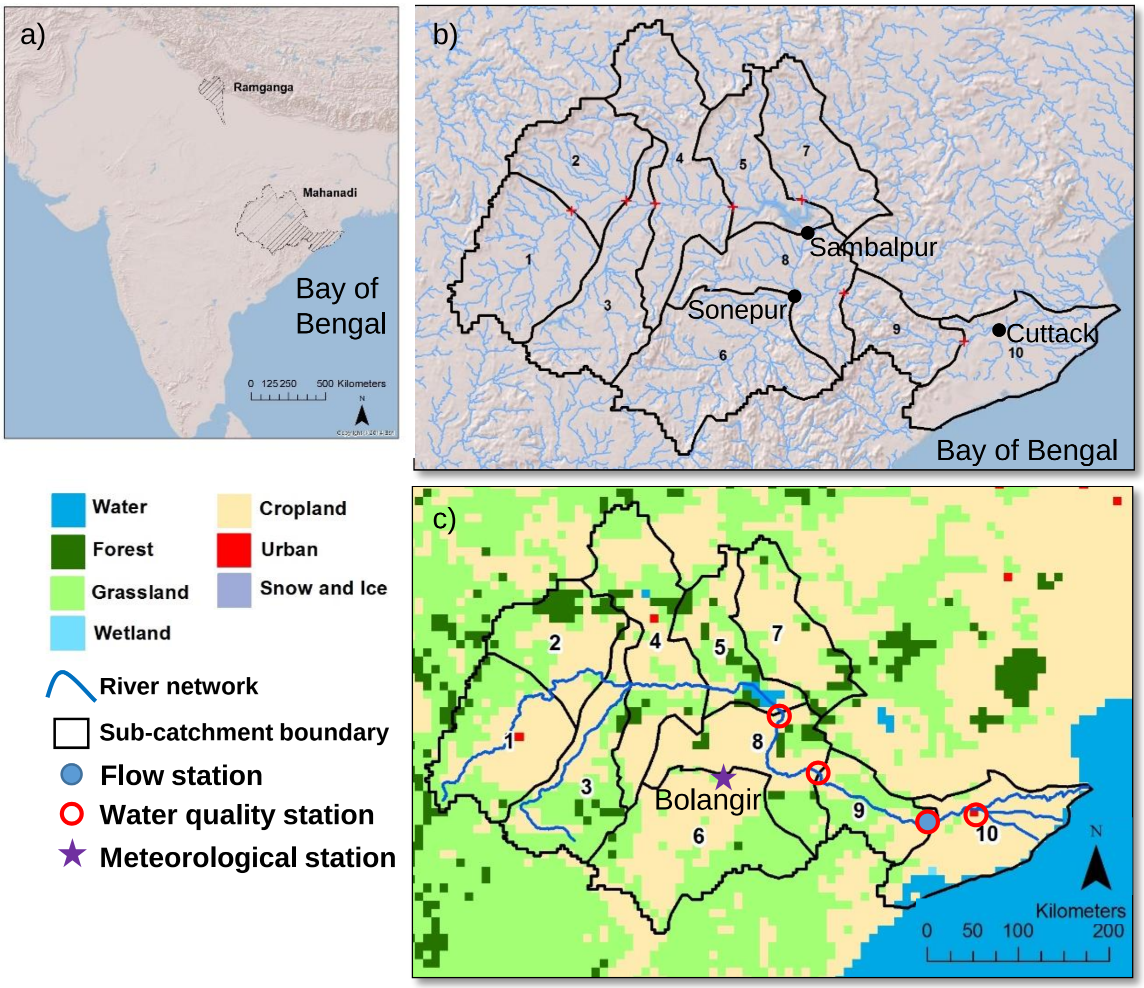

Figure 1 a) A map of Mahanadi river basin in India discharging into Bay of Bengal; b) INCA subcatchments with major cities; c) INCA reaches and associated subcatchment with flow station, water quality modeling stations, metrological station and major land uses.

Table 1 INCA reach and subcatchment characteristic and land use information.

INCA Reach	Subcatchment area (km^2)	Land Use %					
		water	forest	grassland	wetland	cropland	urban
1	17334	0.0	3.3	43.9	0.0	51.9	0.9

2	12798	0.0	14.6	35.4	0.0	50.0	0.0
3	15066	0.0	5.4	48.4	0.0	46.2	0.0
4	19683	0.4	7.0	35.4	0.0	56.8	0.4
5	10044	6.5	14.5	37.1	0.0	41.9	0.0
6	23652	0.0	1.0	40.8	0.0	58.2	0.0
7	12798	0.0	8.9	28.5	0.0	62.7	0.0
8	15066	0.0	7.0	24.2	0.0	68.8	0.0
9	8262	0.0	1.0	54.9	0.0	44.1	0.0
10	15714	9.8	0.0	6.2	0.5	83.0	0.5

For hydrological characteristics, daily precipitation data was measured at the Bolangir meteorological station from 1980 to 2000 which was used as an input to the PERSiST model and INCA models. There are three meteorological stations within the catchment. Bolangir meteorological station was chosen for PERSiST and INCA applications as it has continuous daily rainfall record from 1980 to 2000 and it is also located in the center of the catchment which best represents the overall rainfall condition (Figure 1c). The INCA models uses daily precipitation, SMD, HER and air temperature with the reach characteristics to simulate daily flow at each reach for the entire Mahanadi river system.

The main N and P sources in the Mahanadi River basin include fertilizer application, sewage treatment works (STWs), and atmospheric deposition. Fertilizer application rates are calculated using numbers from Directorate of Agriculture and also are in the similar range to those used in the Ganga studies (Whitehead et al., 2015b). Two main STWs are located near cities of Sambulpur and Cuttack serving populations of 184,000 and 843,402 and discharging 17,000 m^3/day and 132,000 m^3/day of wastewater, respectively (census data 2011) (Draft report of Comprehensive Development Plan, Sambalpur and Final Comprehensive Development Plan for Cuttack Development Plan Area, May, 2011). However there are unaccounted open sewage systems that collect untreated sewage from drains and nullahs or natural watercourses and discharge into rivers. According to the Orissa Pollution Control Board (OSPCB) estimates, the cities in the Mahanadi basin generate about 345,000 m^3/day of raw domestic sewage and these were also included in the model. Atmospheric deposition was assumed to be 6 kg N/ha/year and 0.3 kg P/ha/year which are of similar ranges as the Ganga river basin reflecting the urban and industrial sources of atmospheric N and P (Jin et al., 2015; Whitehead et al., 2015b). Water abstraction rates from irrigation and public water supply along the Mahanadi River have also been estimated and included in the model setup using population numbers and areas of agricultural land.

Flow and water quality data are fairly limited in this study. Daily flow from 1973 to 2012 were obtained at Tikarapada (farthest downstream flow observation station; INCA reach 9 in Figure 1c). Quarterly or monthly NO_3-N and NH_4-N data are available at Tikarapada, Sambalpur (INCA reach 5 in Figure 1c) and Cuttack (INCA reach 10 in Figure 1c) from 2007 and 2014. Monthly total phosphorus (TP) were sampled and measured from 2011 to 2014 at Sonepur (INCA reach 8 in Figure 1c), Tikarapara and Cuttack.

The flow calibration period was selected from 1980 to 2000 when daily rainfall data were measured. Nitrogen and phosphorus calibration period was from 2001 to 2015 based on the availability of observed water quality data.

Climate Data and Bias Correction

In order to model climate and the effects of increasing greenhouse gas concentrations, GCMs have been used widely (IPCC, 2014). However, GCMs cannot provide the high-resolution information for water resources and water quality studies which are typically undertaken at the catchment scale. Therefore RCMs, which are used to dynamically downscale GCM simulations, are used to provide regional climate information such as precipitation, temperature and evaporation rates.

For DECCMA, regional climate data at 25km resolution were obtained for the 1961-2098 period over south Asia downscaled using the PRECIS RCM system (Janes et al., 2018). The focus of this project has been on the global RCP8.5 scenario in order to consider the strongest climate signal with the highest atmospheric greenhouse gas concentrations in the late 21st century (Kebede et al., 2018). Specifically, data were downscaled from RCP8.5 simulations of three different CMIP5 GCMs - CNRM-CM5, GFDL-CM3 and HadGEM2-ES. These GCMs were selected to sample the wide range of future climate changes simulated for northern India under RCP8.5 by the full CMIP5 ensemble. The gridded 25km resolution daily precipitation and temperature data downscaled from these three GCMs were averaged over the Mahanadi River Basin to evaluate the potential impact on flow and water quality from changing climate.

The downscaled CNRM-CM5, GFDL-CM3 and HadGEM2-ES climate data were bias corrected to actual rainfall from 1980 to 1999 for Mahanadi river basin. A standard linear scaling method (Fang et al., 2015) was used for the bias correction of the daily precipitation data, using a 20-year baseline period of 1980 to 1999. Bias correction was also applied in Jin et al. (2018) as part of the DECCMA study with further details (Jin et al., 2018). There were no measured temperature data available during the baseline period. Thus the bias correction of temperature was not feasible in this study.

Finally, the bias corrected daily precipitation and temperature data from climate models were used to calculate hydrologically effective rainfall (HER) and soil moisture deficit (SMD) using the PERSIST model (Futter et al., 2015). The same PERSIST procedures were used as in the Ganga studies (Jin et al., 2015; Whitehead et al., 2015a). Daily HER, temperature and SMD are then used to drive the INCA models.

Socio-Economic Scenarios

Socio-economic changes include population change, industrial development, agriculture and land use change and these affect flow and water quality in river systems. In order to consider socio-economic pathways as a means of integrating social aspects of future changes, one approach is to use the IPCC Shared Socio-economic Pathways (SSPs) strategy. This incorporates 5 broad classifications for future conditions consisting of SSP1 for Sustainability (low mitigation and adaptation challenges), SSP2 for Business as Usual (intermediate mitigation and adaptation challenges), SSP3 for Fragmented World (high mitigation and adaptation challenges), SSP4 for Inequality Rules (high adaptation and low mitigation challenges), and SSP5 for Conventional Development in terms of energy sources (high mitigation and low adaptation challenges) (IPCC, 2014). For DECCMA, three SSP-based scenario narratives have been identified: medium (~SSP2), medium– (~SSP3) and medium+ (~SSP5) that are consistent with the RCP8.5 climate scenario (Kebede et al., 2018). The medium scenarios were regionalization of the SSPs which is necessary for regional impact modelling. The medium- and medium+ scenarios represent low economic growth and high economic growth, respectively. Up to 2050, all three SSPs fall within the band of results compatible with the RCP8.5. Beyond 2050, only SSP5 is consistent with RCP8.5 which can be associated to the highest population growth and highest emissions.

For the Mahanadi River Basin, we focused on population change, effluent discharge, water demand for irrigation and public supply, upgrade of the treatment processes, irrigation change, and atmospheric deposition control.

Population increases vary from state to state and varies depending on assumptions about fertility. In the case of India, the general population is expected to increase by 33%, 58%, and 16% for medium, medium+ and medium- scenarios, respectively at 2050s and to increase by 108% for medium+ scenario at 2090s (Table 2). This is a wide range of population growth and will translate into changes in agriculture, water demand and effluent discharges. Future scenarios from changes in STW discharge rates need to reflect the population changes as well as the implementation of the management plan, which will enhance the capacity and upgrade the treatment of the STWs. Average ammonia and phosphate discharge concentrations are expected to fall from 19mg/L to 5mg/L and from 6mg/L to 1mg/L, respectively under the medium scenario (Table 2). Average phosphorus loads into rivers from STWs should reduce by 86%. Under the medium and medium+ scenarios, the STWs water quality stay at the baseline condition (Table 2).

The demand for public water supply will increase with population growth and changes in agriculture and land use. However, agricultural changes in India are difficult to predict as many factors control the changes. For example, the increasing global population will increase crop prices, which will affect the farmer's reactions to changing prices and then lead to the agricultural expansion. Other factors include potential food scarcity, new improved crop yield, efficient farming which will likely change the agricultural practices. Based on the Food and Agriculture Organization of the United Nations (FAO) estimates, a 22% rise in Kcal/person/day in food production in India is projected by 2050. Therefore, for the purposes of this study we have assumed that the abstraction will increase by 22% on average with a slight variation between scenarios (Table 2).

Atmospheric pollution has become an increasing problem around the world and elevated atmospheric N and P concentrations could alter the terrestrial ecology of plants, natural vegetation and aquatic ecology (Fowler et al., 2013; Hosker and Lindberg, 1982; Phoenix et al., 2012; Swackhamer et al., 2004). In the future, increased industrial development and more intensive farming methods will potentially further increase atmospheric N and P concentrations. In the Ganga's study, N levels were set at 8, 10, and 6 kg N/ha/year at the mid-century for the business as usual, less sustainable future, and more sustainable future scenarios, respectively (Whitehead et al., 2015b). For atmospheric P input, 0.35, 0.175 and 0.5 kg P/ha/year were used for the same scenarios (Jin et al., 2015). In this study, we adopted the range of changes from the Ganga's studies to reflect similar future development in India (e.g urbanization, increased industrial development and intensive farming). N deposition rates are expected to be 8, 10, and 6 kg/ha/year for the three SSPs scenarios (Table 2). The N deposition rate is expected to rise to 15 kg/ha/year for the medium+ scenario at 2090s (Table 2). With regard to the atmospheric P deposition, the changes are 0.35 (medium), 0.5 (medium+), 0.175 (medium-) kg/ha/year at 2050s and 0.75 kg/ha/year for the medium+ scenario at 2090s.

Lastly, projected future agricultural land changes are minor given land in India is already used intensively for growing a wide range of crops (Table 2) (FAO, 2013; Kathpalia and Kapoor, 2010). The highest increase is 10% with the medium+ scenario at the end of the 21st century.

Table 2 A summary of three scenarios for the India Catchments, namely medium, medium+ and medium- for the 2050s and the 2090s.

	2050s			**2090s**
	Medium	**Medium+**	**Medium-**	**Medium+**
Population change	+33%	+58%	+16%	+108%
STW capacity and design for water quality control	flow +33% NH4 at 19mg/L and P at 6 mg/L	flow +58% NH4 at 19mg/L and P at 6 mg/L	flow +16% NH4 at 5mg/L and P at 1 mg/L	flow +108% NH4 at 19mg/L and P at 6 mg/L
Water demand for irrigation and public supply	abstraction +22%	abstraction +25%	abstraction +20%	abstraction +30%

Atmospheric deposition of N	8 kg /ha/year	10 kg /ha/year	6 kg /ha/year	15 kg /ha/year
Atmospheric deposition of P	0.35 kg/ha/year	0.5 kg/ha/year	0.175 kg/ha/year	0.75 kg/ha/year
Intensive agricultural land use change	+5%	+7%	+4%	+10%

Results and Discussions

Flow and INCA model calibration

The river discharge at Tikarapada (farthest downstream observation station) has a wide range of values from a few hundred to about 30,000 m^3/s. The annual river discharge during the baseline period (1980-1999) varied from 23.5 km^3/year to 123 km^3/year with a mean discharge of 47.6±22.5 km^3/year. As a peninsular river, the entire water flows in the Mahanadi basin are controlled by precipitation since there is no major contribution from snowmelt and approximately 85% of total annual water discharge occurs during the monsoon months (from June to October).

A comparison between modeled and observed daily flow shows that INCA simulated daily flow provides an acceptable reproduction of the observed flow with the rising limb of the hydrograph during the onset of monsoon precipitation and the recession curve at the end of the monsoon period (Figure 2). The INCA model catches the overall flow dynamics well, particularly given the complexity and heterogeneity of the Mahanadi river system. The performance statistics of flow during the calibration period at the Tikarapada station are good with r^2 of 0.50 and N-S value of 0.48, which is comparable with other INCA studies for large complex rivers (Jin et al., 2015; Whitehead et al., 2015b) and therefore adequate to represent the flow dynamics of the Mahanadi River.

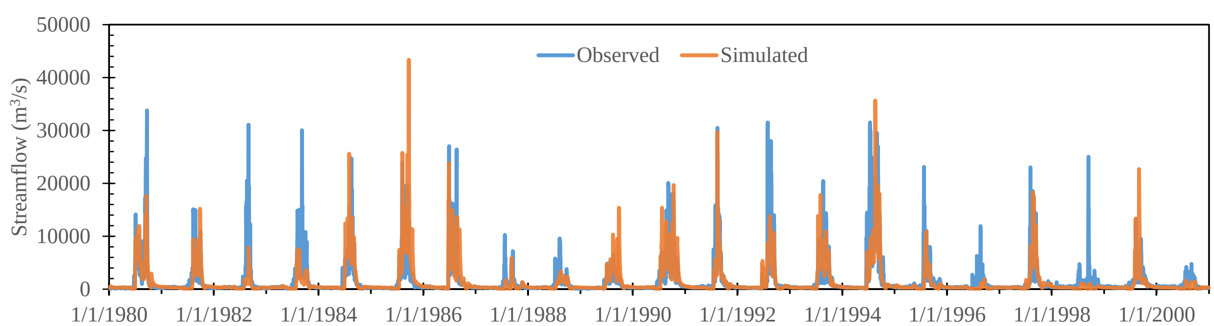

Figure 2 Daily flow calibration at the Tikarapada flow station from 1980 to 2000.

INCA-N and INCA-P model calibration

The water quality models (INCA-N and INCA-P) are much more complicated than the flow model. Nitrogen concentrations in the Mahanadi river basin are controlled by a range of factors such as agricultural farming practices, effluent discharge and atmospheric deposition, as well as nitrogen biochemical processes e.g. nitrification and denitrification in the soils and streams. Phosphorus concentrations are controlled by similar inputs plus the phosphorus processes of absorption and desorption in the soils and river sediments. INCA-N and INCA-P were calibrated from 2001 to 2015 and a summary of model performance statistics is provided in Table 3 and an example of monthly loading is given in Figure 3 at the Tikarapada station of the lower Mahanadi River. INCA-N and INCA-P are able to simulate the seasonal loads of water quality, in which the simulated and observed loads are highly correlated.

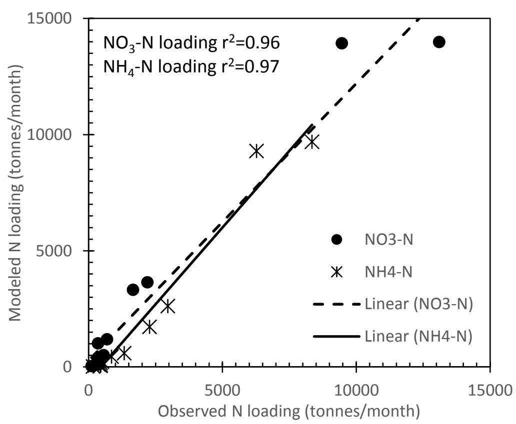

Figure 3 Monthly modeled and observed nitrogen loading (both NO_3-N and NH_4-N) in the Mahanadi River at Tikarapada.

Table 3 Statistical performance summary (r^2) showing the comparison between observed and simulated monthly N and P loading in the Mahanadi river basin.

	TP	NO_3-N	NH_4-N
MA05	0.72	0.9	0.89
MA08	0.68	0.89	0.56
MA09	-	0.56	0.93
MA10	0.46	0.96	0.97

Climate Change Impact on Flow and Water Quality

The future temperatures from the three downscaled climate models indicate rising trends, with the downscaled HadGEM2-ES and GFDL-CM3 models projecting increases of 3°C and 6°C at 2050s and 2090s respectively, while the downscaled CNRM-CM5 model projects smaller increases of 2°C and 4°C at 2050s and 2090s respectively (Figure 4). Temperature rises are throughout the year with smaller increases in the summer (May, June) and greater increases during the rest of the year (Figure 4). Precipitation is also expected to undergo significant changes into the end of the 21st century (Figure 4). During the monsoon months, three downscaled RCM models show increases in precipitation. The downscaled GFDL-CM3 model projects the wettest condition amongst the three climate models at 2090s with 50-70% increases of precipitation from August to October compared to the baseline condition. The downscaled CNRM-CM5 model projected the smallest increases in precipitation toward the end of the century. During non-monsoon period, the precipitation is at a minimum however with some small increases or decreases reflecting the uncertainty of climate scenario projections.

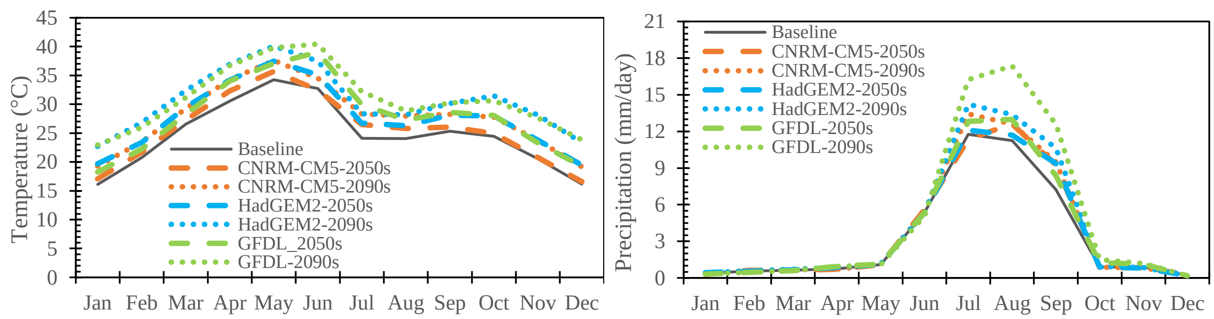

Figure 4 Monthly mean temperature (°C) and precipitation (mm/day) at 2050s and 2090s compared to the baseline condition for the downscaled CNRM-CM5, HadGEM2-ES and GFDL-CM5 climate scenarios.

The projected climate change have the most profound impact on the monsoon high flows (Figure 5). All climate scenarios predicted significant increases in flow from July to November by 2050s and 2090s. Flow increases up to 60% at 2090s under the downscaled GFDL-CM3 scenario reflecting the greater amount of rainfall at the end of the century compared to the baseline (Table 4 and Figure 5). During the non-monsoon season, either increasing or decreasing flow results are seen at 2050s and increases in flow become dominant at 2090s. The future flows show some differences between the three climate scenarios (Table 4) reflecting the variations in future projected precipitation and temperature patterns as this might be expected with the uncertain GCM/RCM model projections. The overall increases in flow could provide additional water for irrigation or water abstraction when needed, however it would also increase the likelihood of flooding which could have significant consequences in India.

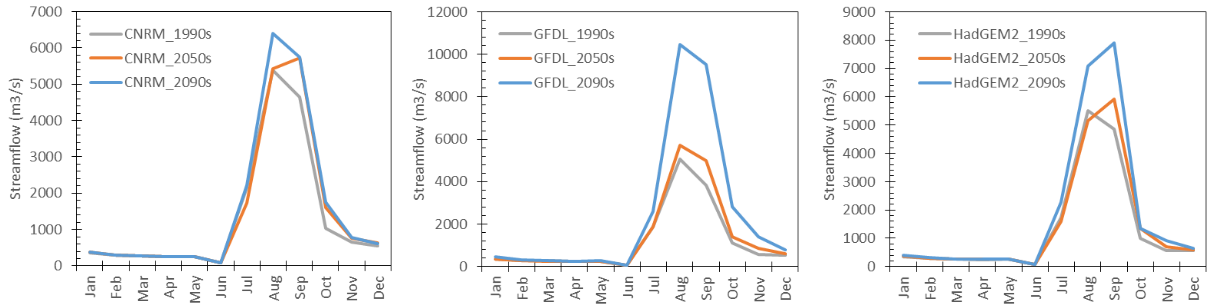

Figure 5 Monthly Mahanadi River flows at baseline, 2050s and 2090s for three climate scenarios.

Table 4 Percentage (%) changes of monthly flow at 2050s and 2090s compared to the baseline for three climate scenarios.

	2050s			2090		
	CNRM-CM5	GFDL-CM3	HadGEM2-ES	CNRM-CM5	GFDL-CM3	HadGEM2-ES
Jan	8.21	5.50	2.98	5.24	21.46	9.67
Feb	2.36	1.73	-0.19	0.98	11.23	3.60
Mar	1.30	-1.33	-0.02	0.89	3.41	2.20
Apr	0.07	-0.07	1.80	0.05	1.87	3.20
May	1.21	-1.37	0.49	-1.14	0.69	-0.81
Jun	-6.49	-1.80	-1.22	-7.49	-0.80	1.17
Jul	-19.82	0.02	-6.92	3.07	28.53	24.00
Aug	0.80	13.04	-6.32	15.86	51.70	22.32
Sep	23.21	31.23	21.69	19.25	59.84	38.51
Oct	56.42	23.59	35.57	41.65	59.99	26.12
Nov	18.68	46.69	22.78	17.14	58.78	37.34
Dec	17.27	9.84	6.08	11.42	32.04	13.87

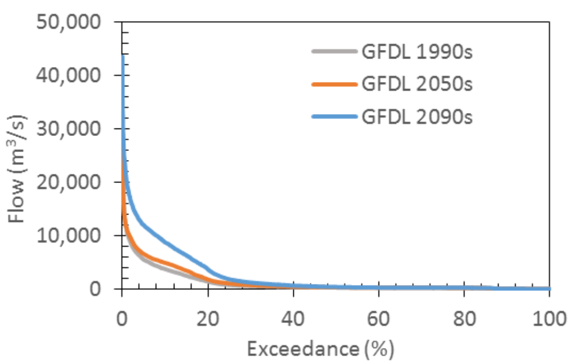

Figure 6 Flow duration curves at 1990s (grey), 2050s (orange) and 2090s (blue) for the mouth of Mahanadi River (MA10) under the downscaled GFDL scenario.

Table 5 Q5 and Q95 flow and % change for flow at MA10 for baseline 1990s, 2050s and 2090s for the three downscaled climate scenarios.

		Flow (m^3/s)			Flow % change	
Climate Scenario	Exceedance	1900s	2050s	2090s	2050s	2090s
CNRM-CM5	Q95	43.7	42.2	41.6	-3.5	-4.8
GFDL-CM3	Q95	46.1	47.2	46.7	2.3	1.2
HadGEM2-ES	Q95	49.2	42.8	44.8	-13.1	-8.9
CNRM-CM5	Q5	6737.0	7268.0	7902.0	7.9	17.3
GFDL-CM3	Q5	5551.0	6586.0	12000.0	18.6	116.2
HadGEM2-ES	Q5	6718.0	7100.0	8895.0	5.7	32.4

The flow duration curves for the Mahanadi River under the climate scenarios illustrate that the high flow distributions are affected significantly by the climate change scenario at 2090s with the Q5 increasing by 116% for the downscaled GFDL-CM3 scenario (Figure 6 and Table 5). The downscaled CNRM-CM5 and HadGEM2-ES scenarios also showed 17% and 32% increases in Q5, respectively. The increases in high flow suggest the potential for increased flooding. Results from this study agreed with previous flow simulations which indicated that an increase in peak runoff in the Mahanadi River outlet will occur in September for the period 2075-2100 (Asokan and Dutta, 2008). Ghosh et al. (2010) also suggested high flow increases in most climate scenarios from 2045-2065. However the low flow distributions do not appear considerably affected. The downscaled CNRM-CM5 and HadGEM2-ES scenarios showed decreases in flow with 5% and 9% changes in Q95 respectively at 2090s, while the downscaled GFDL-CM3 scenario indicated a small increase in Q95 (2%). For the low flow condition, Asokan and Dutta (2008) has suggested more significant decline in flow in dry season (April), while Ghosh et al. (2010) found slight increases in flow (>Q90). It is known that calibration based on the overall fit of flow and goodness-of-fit criterions (r^2 and Nash-Sutcliffe values) has greater uncertainties for the low flow condition than for the high flow condition (Pushpalatha et al., 2012). Therefore careful views must be taken in interpreting the results of low flows and the potential impact to drought condition.

NO_3-N and NH_4-N concentrations are at the lowest in the summer (April-June) when the temperatures are highest. NO_3-N levels vary from 0.2 to 0.3 mg/L and NH_4-N concentrations are generally less than 0.1 mg/L (Figure 7). Increased temperatures and longer residence time in the low flow conditions enhance stronger denitrification and nitrification processes resulting in nitrogen loss and lower NO_3-N and NH_4-N concentrations. The high concentrations of NO_3-N and NH_4-N during the high flow may indicate the quick flush of nitrogen stored in the soil zone. Under changing climate and projected increases in flow, both NO_3-N and NH_4-N concentrations are expected to decrease at 2050s and 2090s for all three climate scenarios. Reductions from the downscaled GFDL-CM3 were highest with approximately 35% reduction at 2050s and 100% at 2090s (Figure 7). The significant decreasing trend in nitrogen reflects both strong reactions and dilution effect.

TP concentrations peak in the summer (May–June) and remain low during the monsoon period primarily due to high flow dilution. Under the climate change, river TP concentrations show decreasing trends at 2050s and 2090s, which is largely due to the increases in the flow and its dilution effect (Figure 7). Greater decreases in P concentrations are seen during the monsoon time compared to the non-monsoon period. The highest TP reduction is 20% and 40% at 2050s and 2090s respectively in the summer under the GFDL-CM3 scenario, which corresponds with the predicted highest flow time (Figure 7). All three scenarios projected similar changes with different extent of reductions.

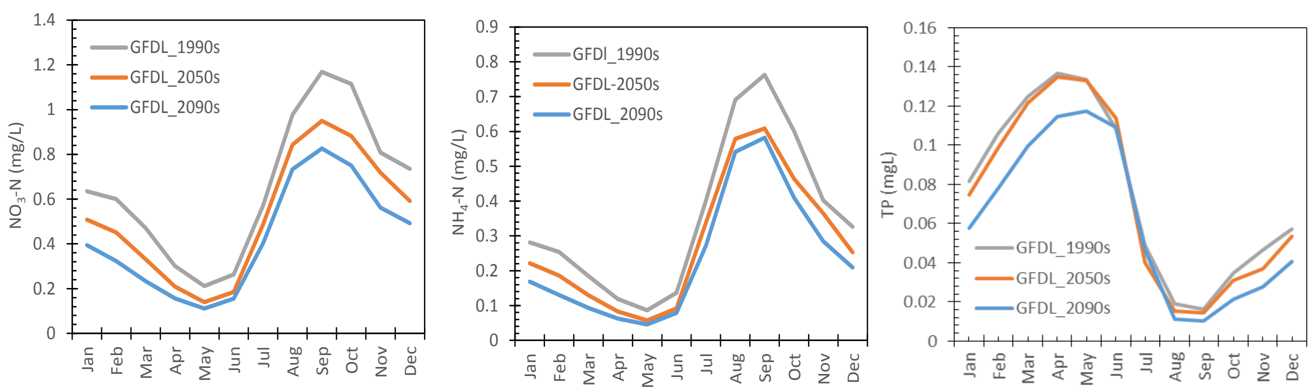

Figure 7 Effects of climate change on monthly mean NO_3-N, NH_4-N and TP concentrations for baseline 1990s (grey), 2050s (orange) and 2090s (blue) under the downscaled GFDL climate scenario.

Combined climate and socio-economic scenario Effects on Flow and Water Quality

The Mahanadi river flows are impacted by future socio-economic conditions with projected decreasing flow for all three SSPs scenarios primarily due to population growth and higher water demand from irrigation and public water supply into the future (Figure 8). The competing relationship between changes induced by climate change and socio-economic change resulted in minor reduction (5% to 7%) at peak flow (August and September). The small percentage changes are due to the high volume of flow. In addition, there seems to be insignificant differences between three socio-economic scenarios (Figure 8), which is because the relatively small changes in simulated abstractions and effluent discharges under different SSPs scenarios relative to the main streamflow of the Mahanadi River.

The water quality simulations show noticeable changes between the scenarios. Due to the reduction in flow, the overall NO_3-N and NH_4-N concentrations would increase from less dilution (Figure 8). Between three SSPs scenarios, lower concentrations of NO_3-N and NH_4-N are seen in the case of the more sustainable scenario (medium-). This reflects the improved wastewater treatment and reduced N from atmospheric deposition. River TP concentrations are predicted to change significantly. For the medium- scenario, TP would reach 80% reduction by 2050s. TP concentrations decrease throughout the year and will be below 0.05 mg/L (Figure 8). This is due to the combined effects from reduced effluent into the rivers with much lower P concentrations, less water abstraction, lower P in atmospheric deposition and better land uses. The water quality control of the wastewater effluent has a major impact on the river water quality. Reduced effluent quantity and lower P concentration in effluent (1 mg/L) will decrease TP concentration by 30–70% by 2050s (Figure 8). The highest reduction occur at the low flow period when wastewater effluent discharge constitutes a larger proportion of the total river flow. During the monsoon months, the reduced effluent with lower P concentrations have less impact to the river TP level (Figure 8). In contrast, TP concentrations show greatest increase under medium+ scenario due to high population, high water demand, high effluent discharge and high P in the atmospheric deposition and high agricultural land uses which all worsen the water quality in the future. Although the concentrations of N and P in the Mahanadi River are lower compared to many other large river systems in developed countries such as the Thames River in UK (Howden et al., 2010; Young et al., 1999) and the Mississippi River in the US (Houser and Richardson, 2010; Mitsch et al., 2001), the increasing N and P could result in profound changes to aquatic ecosystems including eutrophication, algal bloom and associated depletions in dissolved oxygen levels in the rivers and deltaic regions.

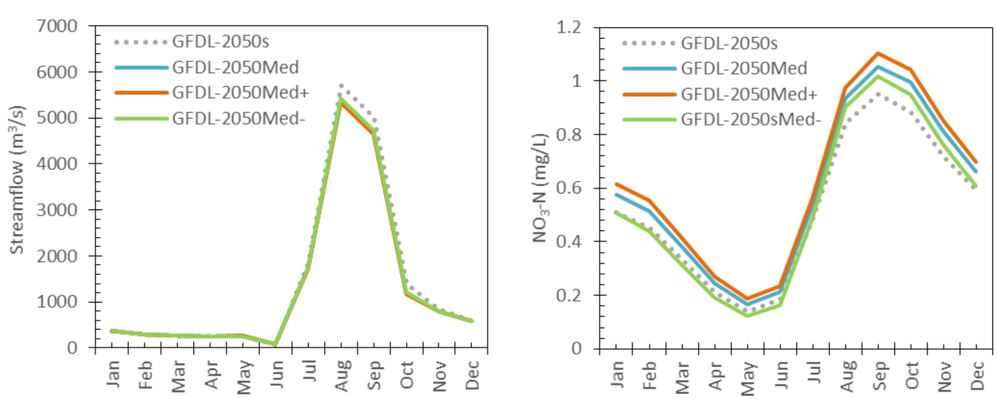

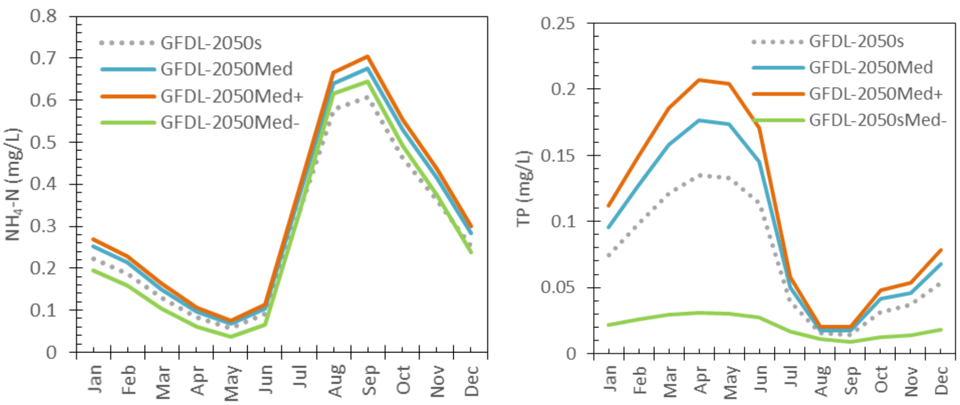

Figure 8 Mean monthly flow, NO_3-N, NH_4-N concentrations at 2050s for the three SSPs (medium, medium+ and medium-) compared to the baseline 1990s (dotted line) under the GFDL-CM3 climate scenario at MA10.

Model uncertainty analysis and limitations

There are a wide range of sources of uncertainty associated with future projections of flow and water quality including choices of GCMs, downscaling technique, choices of hydrological model and water quality model. In this study, three carefully selected GCMs (CNRM-CM5, GFDL-CM3 and HadGEM2-ES) were downscaled to sample the uncertainty in GCM-simulated future climate changes for the region (Janes et al., 2018). PERSiST and INCA models inevitably have uncertainty associated with input and parametrization. For example, spatial distribution of rainfall pattern in the Mahanadi catchment may affect the model performance. In this study, a simple approach was used using data from a single rainfall station and spatially averaged climate data for the whole catchment. As streamflow reflects the integrated response of climatic inputs for the catchment, streamflow calibration at the bottom of the catchment was done carefully to capture the main processes controlling the flow dynamics in the Mahanadi river basin. Although the goodness of fit for downstream flow is satisfactory, given the simplification of the model input, caution is needed when discussing upper reaches/sub-catchments. In addition, there have been extensive studies of uncertainty using the INCA models (Dean et al., 2009; Futter et al., 2007; Jin and Whitehead, 2010; Jin et al., 2012; McIntyre et al., 2005; Rankinen et al., 2002; Wade et al., 2001; Wilby et al., 2006). It has been found that the sensitive parameters related to flow include velocity parameters a and b, groundwater residence time and baseflow index. In addition to flow-related parameters, INCA-N has sensitive parameters related to denitrification process and INCA-P model is sensitive to water column-sediment P exchange and Reach equilibrium P concentration. Therefore identifying sensitive parameters through sensitivity analysis and calibrating models using observed flow and water quality data are essential. Combined uncertainty in future climate and water quality modeling would affect the projection of future changes in flow and water quality as well as the effectiveness of management strategies. While models are helpful for catchment management and planning, the uncertainty and limitation of models should be considered carefully as well as the accuracy of parameter values and outputs from the models should be viewed cautiously. In this study, we have addressed important uncertainties in how large-scale climate conditions and regional socioeconomic factors affecting water flow and quality may change in the future. However, we recognize that other uncertainties have not been addressed. Further work could explore uncertainties relating to the effect of large-scale climate on the climate of the catchment, through using multiple downscaling RCMs, and the translation of climate and socioeconomic factors to flow and water quality data, through using multiple plausible values of parameters in the hydrological modelling.

Conclusions

A simulation of future flows and water quality (N and P) has been conducted for the whole Mahanadi River system using the dynamic process based model INCA. Three most up to date GCMs (CNRM-CM5, GFDL-CM3 and HadGEM2-ES) were selected and downscaled to sample the uncertainty in GCM-simulated future climate changes for India. This modelling study indicates that flow dynamics are largely controlled by the monsoon and current water quality conditions are impacted by land use, sewage effluent discharge and atmospheric deposition. All three climate scenarios consistently indicate an increase in flow during the monsoon period but there are varying flow changes in the dry periods up to 2050s.

The water quality of the Mahanadi River is affected by climate change as the projected increases in rainfall occur in the future and this translates in increased flows and hence enhanced dilution of pollutants. However, as the economy develops and population levels increase in the proposed socio-economic scenarios, water quality will deteriorate, with elevated N and P levels. Some decline in P are anticipated in the case where improved wastewater treatment is introduced.

This study has provided a set of results on the likely future behavior of the Mahanadi River system flow and water quality under climate and socio-economic change scenarios. Simulated flow and water quality data generated at the mouth of the Mahanadi River are crucial for studies which focus on coastal regions downstream.

ACKNOWLEDGEMENTS

The research has been supported by the DECCMA Project on 'DEltas, vulnerability and Climate Change: Migration and Adaptation' which is part of Collaborative Adaptation Research Initiative in Africa and Asia (CARIAA), with financial support from the UK Government's Department for International Development (DfID) and the International Development Research Centre (IDRC), Canada.

References:

2017, Mahanadi River Basin: A Situation Analysis. , *in* Dsouza, C., Joy, K.J., Bhadbhade, N., Bhagat, S., Patil, S., and Jain, S., eds., Forum for Policy Dialogue on Water Conflicts in India, Pune.

Asokan, S.M., and Dutta, D., 2008, Analysis of water resources in the Mahanadi River Basin, India under projected climate conditions: Hydrological Processes, v. 22, p. 3589-3603.

Barlund, I., Rankinen, K., Jarvinen, M., Huitu, E., Veijalainen, N., and Arvola, L., 2009, Three approaches to estimate inorganic nitrogen loading under varying climatic conditions from a headwater catchment in Finland: Hydrology Research, v. 40, p. 167-176.

Bastia, F., and Equeenuddin, S.M., 2016, Spatio-temporal variation of water flow and sediment discharge in the Mahanadi River, India: Global and Planetary Change, v. 144, p. 51-66.

Crossman, J., Futter, M.N., Oni, S.K., Whitehead, P.G., Jin, L., Butterfield, D., Baulch, H.M., and Dillon, P.J., 2013, Impacts of climate change on hydrology and water quality: Future proofing management strategies in the Lake Simcoe watershed, Canada: Journal of Great Lakes Research, v. 39, p. 19-32.

Dean, S., Freer, J., Beven, K., Wade, A.J., and Butterfield, D., 2009, Uncertainty assessment of a process-based integrated catchment model of phosphorus: Stochastic Environmental Research and Risk Assessment, v. 23, p. 991-1010.

Eldeberky, Y., and Hunicke, B., 2015, VULNERABILITY OF THE NILE DELTA TO RECENT AND FUTURE CLIMATE CHANGE: Proceedings of the 36th Iahr World Congress: Deltas of the Future and What Happens Upstream, p. 5061-5067.

Fang, G.H., Yang, J., Chen, Y.N., and Zammit, C., 2015, Comparing bias correction methods in downscaling meteorological variables for a hydrologic impact study in an arid area in China: Hydrol. Earth Syst. Sci., v. 19, p. 2547-2559.

FAO, 2013, The State of Food and Agriculture: World Agriculture Report, Food and Agriculture Organisation, Rome, p. 156.

Flynn, N.J., Paddison, T., and Whitehead, P.G., 2002, INCA Modelling of the Lee System: strategies for the reduction of nitrogen loads: Hydrology and Earth System Sciences, v. 6, p. 467-483.

Fowler, D., Coyle, M., Skiba, U., Sutton, M.A., Cape, J.N., Reis, S., Sheppard, L.J., Jenkins, A., Grizzetti, B., Galloway, J.N., Vitousek, P., Leach, A., Bouwman, A.F., Butterbach-Bahl, K., Dentener, F., Stevenson, D., Amann, M., and Voss, M., 2013, The global nitrogen cycle in the twenty-first century: Philosophical Transactions of the Royal Society B-Biological Sciences, v. 368.

Futter, M.N., Butterfield, D., Cosby, B.J., Dillon, P.J., Wade, A.J., and Whitehead, P.G., 2007, Modeling the mechanisms that control in-stream dissolved organic carbon dynamics in upland and forested catchments: Water Resources Research, v. 43, p. W02424, doi:10.1029/2006WR004960.

Futter, M.N., Erlandsson, M.A., Butterfield, D., Whitehead, P.G., Oni, S.K., and Wade, A.J., 2014, PERSiST: a flexible rainfall-runoff modelling toolkit for use with the INCA family of models: Hydrology and Earth System Sciences, v. 18, p. 855-873.

Futter, M.N., Helliwell, R.C., Hutchins, M., and Aherne, J., 2009, Modelling the effects of changing climate and nitrogen deposition on nitrate dynamics in a Scottish mountain catchment: Hydrology Research, v. 40, p. 153-166.

Futter, M.N., Whitehead, P.G., Sarkar, S., Rodda, H., and Crossman, J., 2015, Rainfall runoff modelling of the Upper Ganga and Brahmaputra basins using PERSiST: Environmental Science-Processes & Impacts, v. 17, p. 1070-1081.

Ghosh, S., Raje, D., and Mujumdar, P.P., 2010, Mahanadi streamflow: climate change impact assessment and adaptive strategies: Current Science, v. 98, p. 1084-1091.

Hadjikakou, M., whitehead, P.G., Jin, L., Futter, M., Hadjinicolaou, P., and Shahgedanova, M., 2011, Modelling nitrogen in the Yeşilirmak River catchment in Northern Turkey: Impacts of future climate and environmental change and implications for nutrient management: Science of the Total Environment, v. 409, p. 2404-2418

Hill, C., Nicholls, R.J., Whitehead, P.W., Dunn, F., Haque, A., Appeaning Addo, K., and Raju, P.V., 2018, Delineating Climate Change Impacts on Biophysical Conditions in Populous Deltas Science of the Total Environment.

Hoang, L.P., Lauri, H., Kummu, M., Koponen, J., van Vliet, M.T.H., Supit, I., Leemans, R., Kabat, P., and Ludwig, F., 2016, Mekong River flow and hydrological extremes under climate change: Hydrology and Earth System Sciences, v. 20, p. 3027-3041.

Hosker, R.P., and Lindberg, S.E., 1982, REVIEW - ATMOSPHERIC DEPOSITION AND PLANT ASSIMILATION OF GASES AND PARTICLES: Atmospheric Environment, v. 16, p. 889-910.

Houser, J.N., and Richardson, W.B., 2010, Nitrogen and phosphorus in the Upper Mississippi River: transport, processing, and effects on the river ecosystem: Hydrobiologia, v. 640, p. 71-88.

Howden, N.J.K., Burt, T.P., Worrall, F., Whelan, M.J., and Bieroza, M., 2010, Nitrate concentrations and fluxes in the River Thames over 140 years (1868-2008): are increases irreversible?: Hydrological Processes, v. 24, p. 2657-2662.

Immerzeel, W., 2008, Historical trends and future predictions of climate variability in the Brahmaputra basin: International Journal of Climatology, v. 28, p. 243-254.

IPCC, 2007, Climate Change 2007: The Physical Science Basis: Summary for Policymakers. Fourth Assessment Report of the Intergovernmental Panel on Climate Change, Parry, M.L., Canziani, O.F., Palutikof, J.P., van der Linden, P.J. and Hanson, C.E. Eds., Cambridge University Press, Cambridge, UK,.

IPCC, 2013, Summary for Policymakers. In: Climate Change 2013: The Physical Science Basis. Contribution of Working Group I to the Fifth Assessment Report of the Intergovernmental Panel on Climate Change: [Stocker, T.F., D. Qin, G.-K. Plattner, M. Tignor, S.K. Allen, J. Boschung, A. Nauels, Y. Xia, V. Bex and P.M. Midgley (eds.)]. Cambridge University Press, Cambridge, United Kingdom and New York, NY, USA.

IPCC, 2014, Summary for Policymakers. In: Climate Change 2014 Mitigation of Climate Change Working Group III Contribution to the Fifth Assessment Report of the Intergovernmental Panel on Climate Change: Cambridge, Cambridge Univ Press.

Jackson-Blake, L.A., Wade, A.J., Futter, M.N., Butterfield, D., Couture, R.M., Cox, B.A., Crossman, J., Ekholm, P., Halliday, S.J., Jin, L., Lawrence, D.S.L., Lepisto, A., Lin, Y., Rankinen, K., and Whitehead, P.G., 2016, The INtegrated CAtchment model of phosphorus dynamics (INCA-P): Description and demonstration of new model structure and equations: Environmental Modelling & Software, v. 83, p. 356-386.

Janes, T., McGrath, F., Macadam, I., and Jones, R., 2018, High-resolution climate projections for South Asia to inform climate impacts and adaptation studies in the Ganges-Brahmaputra-Meghna and Mahanadi deltas: Science of the Total Environment.

Jarvie, H.P., Wade, A.J., Butterfield, D., Whitehead, P.G., Tindall, C.I., Virtue, W.A., Dryburgh, W., and McGraw, A., 2002, Modelling nitrogen dynamics and distributions in the River Tweed, Scotland: an application of the INCA model: Hydrology and Earth System Sciences, v. 6, p. 433-453.

Jin, L., Whitehead, P., Siegel, D.I., and Findlay, S., 2011, Salting our landscape: An integrated catchment model using readily accessible data to assess emerging road salt contamination to streams: Environmental Pollution, v. 159, p. 1257-1265.

Jin, L., and Whitehead, P.G., 2010, Modeling Flow and Nitrogen Dynamics in the River Thames: Implication of Future Climate Induced Water Vulnerability in Southeast England: British Hydrological Society International Conference Proceedings, Newcastle, p. pp 21.

Jin, L., Whitehead, P.G., Appeaning Addo, K., Amisigo, B., Macadam, I., Janes, T., Crossman, J., Nicholls, R.J., McCartney, M., and Rodda, H.J.E., 2018, Modelling Future Flows of the Volta River System: Impacts of Climate Change and Socio-Economic Changes Science of the Total Environment, v. DECCMA Special Issue.

Jin, L., Whitehead, P.G., Futter, M.N., and Lu, Z.L., 2012, Modelling the impacts of climate change on flow and nitrate in the River Thames: assessing potential adaptation strategies: Hydrology Research, v. 43, p. 902-916.

Jin, L., Whitehead, P.G., Heppell, C.M., Lansdown, K., Purdie, D.A., and Trimmer, M., 2016, Modelling flow and inorganic nitrogen dynamics on the Hampshire Avon: Linking upstream processes to downstream water quality: Science of the Total Environment, v. 572, p. 1496-1506.

Jin, L., Whitehead, P.G., Sarkar, S., Sinha, R., Futter, M.N., Butterfield, D., Caesar, J., and Crossman, J., 2015, Assessing the impacts of climate change and socio-economic changes on flow and phosphorus flux in the Ganga river system: Environmental Science-Processes & Impacts, v. 17, p. 1098-1110.

Kathpalia, G.N., and Kapoor, R., 2010, Management of Land and other Resources for Inclusive Growth: India 2050: Alternative Futures, Dehli, p. 32.

Kay, S., Caesar, J., Wolf, J., Bricheno, L., Nicholls, R.J., Islam, A., Haque, A., Pardaens, A., and Lowe, J.A., 2015, Modelling the increased frequency of extreme sea levels in the Ganges-Brahmaputra-Meghna delta due to sea level rise and other effects of climate change: Environmental Science-Processes & Impacts, v. 17, p. 1311-1322.

Kebede, A.S., Nicholls, R.J., Allan, A., Arto, I., Cazcarro, I., Fernandes, J.A., Hill, C.T., Hutton, C.W., Kay, S., Lazar, A.N., Macadam, I., Palmer, M., Suckall, N., Tompkins, E.L., Vincent, K., and Whitehead, P.G., 2018, Applying the Global RCP–SSP–SPA Scenario Framework at Sub-National Scale: A Multi-Scale and Participatory Scenario Approach: Science of the Total Environment, v. DECCMA Special Issue.

Lazar, A.N., Butterfield, D., Futter, M.N., Rankinen, K., Thouvenot-Korppoo, M., Jarritt, N., Lawrence, D.S.L., Wade, A.J., and Whitehead, P.G., 2010, An assessment of the fine sediment dynamics in an upland river system: INCA-Sed modifications and implications for fisheries: Science of the Total Environment, v. 408, p. 2555-2566.

Lazar, A.N., Clarke, D., Adams, H., Akanda, A.R., Szabo, S., Nicholls, R.J., Matthews, Z., Begum, D., Saleh, A.F.M., Abedin, M.A., Payo, A., Streatfield, P.K., Hutton, C., Mondal, M.S., and Moslehuddin, A.Z.M., 2015, Agricultural livelihoods in coastal Bangladesh under climate and environmental change - a model framework: Environmental Science-Processes & Impacts, v. 17, p. 1018-1031.

Lu, Q., Whitehead, P.G., Bussi, G., Futter, M.N., and Nizzetto, L., 2017, Modelling metaldehyde in catchments: a River Thames case-study: Environmental Science-Processes & Impacts, v. 19, p. 586-595.

McIntyre, N., Jackson, B., Wade, A.J., Butterfield, D., and Wheater, H.S., 2005, Sensitivity analysis of a catchment-scale nitrogen model: Journal of Hydrology, v. 315, p. 71-92.

Mitsch, W.J., Day, J.W., Gilliam, J.W., Groffman, P.M., Hey, D.L., Randall, G.W., and Wang, N.M., 2001, Reducing nitrogen loading to the Gulf of Mexico from the Mississippi River Basin: Strategies to counter a persistent ecological problem: Bioscience, v. 51, p. 373-388.

Nicholls, R.J., Hutton, C.W., Lazar, A.N., Allan, A., Adger, W.N., Adams, H., Wolf, J., Rahman, M., and Salehin, M., 2016, Integrated assessment of social and environmental sustainability dynamics in the Ganges-Brahmaputra-Meghna delta, Bangladesh: Estuarine Coastal and Shelf Science, v. 183, p. 370-381.

Phoenix, G.K., Emmett, B.A., Britton, A.J., Caporn, S.J.M., Dise, N.B., Helliwell, R., Jones, L., Leake, J.R., Leith, I.D., Sheppard, L.J., Sowerby, A., Pilkington, M.G., Rowe, E.C., Ashmorek, M.R., and Power, S.A., 2012, Impacts of atmospheric nitrogen deposition: responses of multiple plant and soil parameters across contrasting ecosystems in long-term field experiments: Global Change Biology, v. 18, p. 1197-1215.

Pushpalatha, R., Perrin, C., Le Moine, N., and Andreassian, V., 2012, A review of efficiency criteria suitable for evaluating low-flow simulations: Journal of Hydrology, v. 420, p. 171-182.

Rankinen, K., Lepisto, A., and Granlund, K., 2002, Sensitivity of the INCA model to N process parameters and hydrological input In: Jakeman, A.J., Rizzoli, A.E. (Eds.), IEMSS 2002 Proceedings IEMSS Conference Lugano, vol. 1, pp. 317-320.

Ranzini, M., Forti, M.C., Whitehead, P.G., Arcova, F.C.S., de Cicco, V., and Wade, A.J., 2007, Integrated Nitrogen CAtchment model (INCA) applied to a tropical catchment in the Atlantic Forest, Sao Paulo, Brazil: Hydrology and Earth System Sciences, v. 11, p. 614-622.

Rao, P.G., 1995, the effect of climate change on streamflows in the Mahanadi River Basin, India: Water International, v. 20, p. 205-212.

Sherif, M.M., and Singh, V.P., 1999, Effect of climate change on sea water intrusion in coastal aquifers: Hydrological Processes, v. 13, p. 1277-1287.

Smajgl, A., Toan, T.Q., Nhan, D.K., Ward, J., Trung, N.H., Tri, L.Q., Tri, V.P.D., and Vu, P.T., 2015, Responding to rising sea levels in the Mekong Delta: Nature Climate Change, v. 5, p. 167-U167.

Susnik, J., Vamvakeridou-Lyroudia, L.S., Baumert, N., Kloos, J., Renaud, F.G., Jeunesse, I., Mabrouk, B., Savic, D.A., Kapelan, Z., Ludwig, R., Fischer, G., Roson, R., and Zografos, C., 2015, Interdisciplinary assessment of sea-level rise and climate change impacts on the lower Nile delta, Egypt: Science of the Total Environment, v. 503, p. 279-288.

Swackhamer, D.L., Paerl, H.W., Eisenreich, S.J., Hurley, J., Hornbuckle, K.C., McLachlan, M., Mount, D., Muir, D., and Schindler, D., 2004, Impacts of Atmospheric Pollution on Aquatic Ecosystems: Issues in Ecology.

Van, P.D.T., Popescu, I., van Griensven, A., Solomatine, D.P., Trung, N.H., and Green, A., 2012, A study of the climate change impacts on fluvial flood propagation in the Vietnamese Mekong Delta: Hydrology and Earth System Sciences, v. 16, p. 4637-4649.

Vastila, K., Kummu, M., Sangmanee, C., and Chinvanno, S., 2010, Modelling climate change impacts on the flood pulse in the Lower Mekong floodplains: Journal of Water and Climate Change, v. 1, p. 67-86.

Wade, A.J., Durand, P., Beaujouan, V., Wessel, W.W., Raat, K.J., Whitehead, P.G., Butterfield, D., Rankinen, K., and Lepisto, A., 2002, A nitrogen model for European catchments: INCA, new model structure and equations: Hydrology and Earth System Sciences, v. 6, p. 559-582.

Wade, A.J., Hornberger, G.M., Whitehead, P.G., Jarvie, H.P., and Flynn, N., 2001, On modeling the mechanisms that control in-stream phosphorus, macrophyte, and epiphyte dynamics: An assessment of a new model using general sensitivity analysis: Water Resources Research, v. 37, p. 2777-2792.

Walling, D.E., 1997, The response of sediment yields to environmental change, *in* Walling, D.E., and Probst, J.L., eds., Human Impact on Erosion and Sedimentation: Iahs Publication, p. 77-89.

Walling, D.E., and Fang, D., 2003, Recent trends in the suspended sediment loads of the world's rivers: Global and Planetary Change, v. 39, p. 111-126.

Whitehead, P.G., Barbour, E., Futter, M.N., Sarkar, S., Rodda, H., Caesar, J., Butterfield, D., Jin, L., Sinha, R., Nicholls, R., and Salehin, M., 2015a, Impacts of climate change and socio-economic scenarios on flow and water quality of the Ganges, Brahmaputra and Meghna (GBM) river systems: low flow and flood statistics: Environmental Science-Processes & Impacts, v. 17, p. 1057-1069.

Whitehead, P.G., Butterfield, D., and Wade, A.J., 2009, Simulating metals and mine discharges in river basins using a new integrated catchment model for metals: pollution impacts and restoration strategies in the Aries-Mures river system in Transylvania, Romania: Hydrology Research, v. 40, p. 323-346.

Whitehead, P.G., Jin, L., Baulch, H.M., Butterfield, D.A., Oni, S.K., Dillon, P.J., Futter, M., Wade, A.J., North, R., O'Connor, E.M., and Jarvie, H.P., 2011, Modelling phosphorus dynamics in multi-branch river systems: A study of the Black River, Lake Simcoe, Ontario, Canada: Science of the Total Environment, v. 412, p. 315-323.

Whitehead, P.G., Sarkar, S., Jin, L., Futter, M.N., Caesar, J., Barbour, E., Butterfield, D., Sinha, R., Nicholls, R., Hutton, C., and Leckie, H.D., 2015b, Dynamic modeling of the Ganga river system: impacts of future climate and socio-economic change on flows and nitrogen fluxes in India and Bangladesh: Environmental Science-Processes & Impacts, v. 17, p. 1082-1097.

Whitehead, P.G., Wilson, E.J., Butterfield, D., and Seed, K., 1998, A semi-distributed integrated flow and nitrogen model for multiple source assessment in catchments (INCA): Part II - application to large river basins in south Wales and eastern England: Science of the Total Environment, v. 210, p. 559-583.

Wilby, R.L., Whitehead, P.G., Wade, A.J., Butterfield, D., Davis, R.J., and Watts, G., 2006, Integrated modelling of climate change impacts on water resources and quality in a lowland catchment: River Kennet, UK: Journal of Hydrology, v. 330, p. 204-220.

Young, K., Morse, G.K., Scrimshaw, M.D., Kinniburgh, J.H., MacLeod, C.L., and Lester, J.N., 1999, The relation between phosphorus and eutrophication in the Thames Catchment, UK: Science of the Total Environment, v. 228, p. 157-183.